

Supramolecular Approach to Electron Paramagnetic Resonance Distance Measurement of Spin-Labeled Proteins

*Zhimin Yang,[†] Richard A. Stein,[‡] Thacien Ngendahimana,[§] Maren Pink,[⊥] Suchada Rajca,[†]
Gunnar Jeschke,^{*†} Sandra S. Eaton,^{*§} Gareth R. Eaton,[§] Hassane S. Mchaourab,^{*‡} and Andrzej
Rajca^{*†}*

[†]Department of Chemistry, University of Nebraska, Lincoln, Nebraska 68588-0304.

[‡]Department of Molecular Physiology and Biophysics, Vanderbilt University, Nashville,
Tennessee 37232.

[§]Department of Chemistry and Biochemistry, University of Denver, Denver, Colorado 80208.

[⊥]IUMSC, Department of Chemistry, Indiana University, Bloomington, Indiana 47405-7102.

[†]ETH Zürich, Department of Chemistry and Applied Biosciences, Vladimir-Prelog-Weg 2, CH-
8093 Zürich, Switzerland.

AUTHOR INFORMATION

*** Corresponding Authors:** arajca1@unl.edu, hassane.mchaourab@Vanderbilt.Edu,
sandra.eaton@du.edu, gjeschke@ethz.ch

ABSTRACT

We demonstrate a host-guest molecular recognition approach to advance double electron-electron resonance (DEER) distance measurements of spin-labeled proteins. We synthesized an iodoacetamide (IA) derivative of 2,6-diazaadamantane nitroxide (DZD) spin label that could be doubly incorporated into T4 Lysozyme (T4L) by site-directed spin labeling (SDSL) with efficiency up to 50% per cysteine. The rigidity of the fused ring structure and absence of mobile methyl groups increase the spin echo dephasing time (T_m) at temperatures above 80 K. This enables DEER measurements of distances >4 nm in DZD labeled-T4L in glycerol/water at temperatures up to 150 K, with increased sensitivity compared to common spin label such as MTSL. Addition of β -cyclodextrin (β -CD) reduces the rotational correlation time of the label, slightly increases T_m , and most importantly, narrows (and slightly lengthens) the inter-spin distance distributions. The distance distributions are in good agreement with simulated distance distributions obtained by rotamer libraries. These results provide a foundation for developing supramolecular recognition to facilitate long-distance DEER measurements at near physiological temperatures.

KEYWORDS. Host-guest systems • Cyclodextrins • EPR spectroscopy • Biophysics • Radicals

Introduction

Nitroxide spin labels are useful probes for investigation of biomolecules.¹ SDSL-DEER has the advantages of high sensitivity, large distance range, and absolute distance distributions.¹⁻⁶ The most widely used spin label for SDSL-DEER is methane thiosulfonate pyrrolidine nitroxide (MTSL, Figure 1), which selectively reacts with cysteine that can be introduced at selected locations by site directed mutagenesis.^{1,7} The *gem*-dimethyl groups in MTS defense the temperatures at which these measurements can be made, because the T_m , the major factor limiting sensitivity and the range of distances, is shortened by the dynamic averaging effects associated with the methyl group rotation at ≥ 80 K.⁸ Recently, distance measurements at room temperature were demonstrated using a new generation of nitroxide spin labels devoid of methyl groups, iodoacetamide spirocyclohexyl pyrimidine nitroxide (IA-Spiro, Figure 1).⁹ T4 Lysozyme (T4L) doubly spin-labeled with Spiro nitroxide possesses sufficiently long T_m at Q-band, to allow measurement of 4-nm distances at 160 K in glycerol/water and 3-nm distances at room temperature in a trehalose matrix.^{9a}

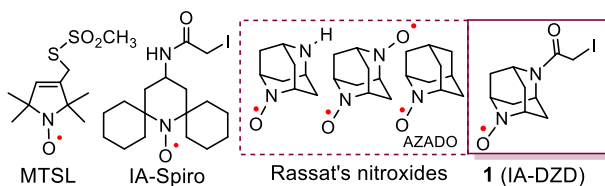


Figure 1. Structures of nitroxide radicals and spin labels.

Adamantane was pioneered as the framework for stable nitroxide radicals by Rassat.¹⁰ These nitroxides have small molecular size and rigid structure, which are highly desirable in the design of a spin label with long T_m . In addition, adamantane and its derivatives complex strongly to β -cyclodextrin (β -CD), with large association constants, $K_a \approx 10^3 - 10^6$ M⁻¹.¹¹ Bagryanskaya and

coworkers reported the measurement of electron spin relaxation time $T_2 \approx T_m \approx 1.2 \mu\text{s}$ for triplet excited state benzophenone encapsulated inside methylated β -CD in water/glycerol at 30 K. Notably, this T_m was longer by a factor of 3 – 4, compared to that of benzophenone in toluene.¹²

We envision a novel supramolecular approach, taking advantage of host–guest molecular recognition, to lengthen the T_m of spin-labeled proteins and decrease conformational mobility. Binding of β -CD to spin labels at solvent exposed sites of a protein would increase T_m and this may facilitate long-distance DEER measurements at near physiological temperatures.

Materials and Methods

X-ray crystallography. Crystals of **1** were obtained by slow evaporation from a pentane/chloroform solvent mixture. Data were collected at 173 K using $Mo\text{ }K\alpha$ radiation and integrated (SAINT).¹³ Intensity data were corrected for absorption (SADABS).¹⁴ The structure was solved with intrinsic methods (SHELXT)^{15a} and refined on $F2$ (SHELXL).^{15b} Crystal data for **1**: $C_{10}H_{14}IN_2O_2$, $M_r = 321.13 \text{ g mol}^{-1}$, yellow block, $0.24 \times 0.23 \times 0.1 \text{ mm}$, orthorhombic, $Pbca$, $a = 8.3415(4) \text{ \AA}$, $b = 10.1215(4) \text{ \AA}$, $c = 25.9996(12) \text{ \AA}$, $V = 2195.11(17) \text{ \AA}^3$, $Z = 8$, $\mu(Mo\text{ }K\alpha) = 2.900 \text{ mm}^{-1}$, $\theta_{\max} = 30.04^\circ$, 20,397 reflections measured, 3216 independent ($R_{\text{int}} = 0.0917$), $R1 = 0.0172$ [$I > 2\sigma(I)$], $wR2 = 0.0694$ (all data), residual density peaks: 0.694 to $-0.859 \text{ e \AA}^{-3}$. Additional crystal and structure refinement data for **1** are in the Supporting Information and the accompanying file in CIF format.

Synthesis. Standard techniques for synthesis under inert atmosphere (argon or nitrogen), using custom-made Schlenk glassware and custom-made double manifold high vacuum lines, were employed. Chromatographic separations were carried out using normal phase neutral alumina or silica gel.

Preparation of 3 (via intermediate 2): To a cooled suspension of *N*-chlorosuccinimide (NCS, 0.3393 g, 2.54 mmol) in Et₂O (40 mL) was added *endo*-3-amino-9-methylazabicyclo[3.3.1]nonane (0.200 g, 1.30 mmol) dropwise while stirring. After 5 minutes in an ice-bath, trimethylamine (0.514 mg, 5.08 mmol) was added, the suspension was immediately irradiated with mercury lamp (200 W) under nitrogen atmosphere for 3.5 h. The mixture was filtered, and the white solid was collected (0.307 g). This crude mixture was used directly for preparation of 3.

To the solution of crude mixture containing amine **2** (100 mg) in dichloromethane (DCM, 2.2 mL) was added triethylamine (Et₃N, 193.3 mg, 1.91 mmol) under a nitrogen atmosphere. The mixture was cooled in an ice-bath and chloroacetyl chloride (84.71 mg, 0.75 mmol) in DCM (0.8 mL) was added dropwise to the stirred mixture at 0 °C; the solution became dark gradually within 5 min. The mixture was stirred overnight at room temperature. The brown suspension was concentrated by reduced-pressure evaporation and diluted with 5 mL saturated NaHCO₃. The resulting mixture was extracted by DCM (3×5 mL). The combined extracts were dried over Na₂SO₄ and concentrated by vacuum. The residue was purified by silica gel chromatography using 10:1 ethyl acetate (EA)/Et₃N to give a white solid. *R*_f 0.2 (silica, 9:1 EA/ Et₃N). M.p. (dec) 70 °C, measured under N₂, forming dimer (see: SI). ¹H NMR (400 MHz, CDCl₃): δ 4.837 (br, 1H), 4.123 (br, 1H), 4.037 (s, 2H), 2.983 (br, 2H), 2.571 (s, 3H), 2.136 (t, 4H), 1.774 (d, *J*=12.4 Hz), 1.653 (d, *J*=12.8 Hz). ¹³C NMR (CDCl₃, 100 MHz): δ 163.7 (1 CO), 51.7 (2 CH), 49.3 (1 CH₂Cl), 44.0 (1 CH₃), 41.25 (1 CH from the ring), 41.18 (1 CH from the ring), 32.3 (2 CH from the ring), 30.65 (2 CH₂ from the ring). IR (ZnSe, cm⁻¹): 2925, 1635, 1438, 1416, 1375, 1234, 1062, 780, 714. LRMS-ESI (0.1% HCOOH in MeOH) m/z: [M + 1 H]⁺ calcd for C₁₁H₁₈ClN₂O 229.1108, found 229.5. HRMS-ESI m/z: calcd for C₁₁H₁₇ClN₂O 228.1029, found 228.1027.

Preparation of amine hydrochloride 4: Chloro-acetamide amine **3** (53.4 mg, 0.23 mmol) was transferred into Schlenk, dried under high vacuum line overnight and charged with N₂ gas before adding another reagent. The solution of 1-chloroethyl chloroformate (ACE-Cl, 36.47 mg, 0.25 mmol) in anhydrous 1,2-DCE (0.27 mL), which was prepared in a N₂ bag, was added dropwise into Schlenk vessel under N₂ at 0 °C to give yellow suspension. The yellow suspension was stirred for a further 30 min at 0 °C before it was warmed to room temperature. Once at room temperature, the mixture was heated to 80 °C for 3 h. After cooling to room temperature, the yellow suspension was concentrated by reduced-pressure evaporation and the residue was re-dissolved in MeOH (0.14 mL) to give yellow solution and heated for additional 2 h at 80–85 °C. After cooling to room temperature, the solvents were removed by rotavapor and the crude was dried under high vacuum line overnight to give off-white solid (59.0 mg, 100%). ¹H NMR (300 MHz, CDCl₃): δ 5.006 (br, 1H), 4.295 (br, 1H), 4.062 (s, 2H), 3.945 (br, 2H), 2.542 (d, *J* = 12.9 Hz), 2.458 (d, *J* = 12.9 Hz), 2.096 (d, *J* = 13.5 Hz), 2.004 (d, *J* = 13.2 Hz). ¹³C NMR (176 MHz, CDCl₃): δ 164.3, δ 47.0, δ 46.5, δ 41.6, δ 40.7, δ 32.3, δ 31.5. IR (ZnSe, cm⁻¹): 3396, 2950, 1641, 1431, 1241, 1099. Mp 245–250 °C. LRMS-ESI (0.1% HCOOH in MeOH) m/z: [M + H]⁺ calcd for C₁₀H₁₆ClN₂O 215.0591, found 215.1. HRMS-ESI m/z: calcd for C₁₀H₁₅ClN₂O 214.0873, found 214.0865

Preparation of nitroxide 5: Hydrochloride amine **4** was evenly divided into 5 vials, of which each contained 23.6 mg. To the suspension of each aliquot of hydrochloride amine **4** (23.6 mg), NaHCO₃ (29.7 mg) and NaWO₄·2H₂O (4.6 mg) in MeOH (830 μL), PhCN (116 μL) was added. Vials were covered with aluminum foil and cooled to 0 °C. Subsequently, H₂O₂ (35 wt. %, 165.2 μL) was added dropwise within 2 min at 0 °C, and then the reaction mixture was warmed to room temperature. Following vigorous stirring at room temperature for 6.5 h, the solvents were removed by N₂ gas flow, to give a mixture of white and yellow solid. The combined crude mixture was

purified by neutral aluminum oxide chromatography using ethyl acetate to give yellow solid (77 mg, 72%). R_f 0.35 (neutral alumina, ethyl acetate). Mp (dec) 130–131 °C, measured under N₂ atmosphere. IR (ZnSe, cm⁻¹): 2952, 2912, 1646, 1436, 1072, 1029, 781. LRMS-ESI (0.1% HCOOH in MeOH) m/z: [M + 2 H]⁺ calcd for C₁₀H₁₆ClN₂O₂ 231.0900, found 231.3. HRMS-ESI m/z: calcd for C₁₀H₁₄ClN₂O₂ 229.0744, found 229.0751.

Preparation of spin label 1: NaI (41 mg, 0.27 mmol) was dried under high vacuum line at 60 °C overnight. Nitroxide **5** (6.27 mg, 0.027 mmol) was transferred into Schlenk by dichloromethane and dried under high vacuum line at 40 °C overnight. NaI was added into Schlenk in a N₂-filled bag, followed by anhydrous acetone (about 1 mL) via vacuum transfer, to give a yellow solution. The Schlenk was covered with aluminum foil and was heated to 40 °C for 5–6 h. Because R_f -values of **5** and **1** are identical on neutral alumina, the reaction was monitored by LR MS (ESI). Acetone was removed by N₂ gas flow, to give a mixture of white and yellow solid. The crude mixture was purified by neutral aluminum oxide chromatography using ethyl acetate to give yellow solid (4.74 mg, 55%). R_f 0.35 (neutral aluminum oxide, ethyl acetate). Mp (dec) 101–102 °C, measured under N₂ atmosphere. IR (ZnSe, cm⁻¹): 2952, 2921, 1650, 1441, 1415, 1086, 735. LRMS-ESI (0.1% HCOOH in MeOH) m/z: [M + 2 H]⁺ calcd for C₁₀H₁₆IN₂O₂ 323.0256, found 323.6. HRMS-ESI m/z: calcd for C₁₀H₁₄IN₂O₂ 321.0100, found 321.0096.

Spin labeling of T4L. Sample labeling was carried out as previously described.^{16,17} Briefly, T4L mutants were expressed in K38 cells in Luria Broth (LB) and purified using cation exchange chromatography. Labeling of the mutants was initiated by adding an excess of spin-label and incubating for 2 hours at room temperature, a second addition of spin-label was made and the samples incubated overnight at 4 °C. The samples were then desalting and concentrated.

Electron spin relaxation studies. Field-swept echo detected spectra and relaxation times were recorded at X-band and Q-band on a Bruker E580 equipped with an Oxford ESR935 cryostat and a Bruker X-band ER4118X-MS5 split ring resonator or Q-band ER5107D2 resonator. The length of a $\pi/2$ pulse was 20 ns at X-band and 40 ns at Q-band. Field-swept echo-detected spectra were obtained with a two-pulse $\pi/2-\tau-\pi-\tau$ -echo sequence and 2-pulse phase cycling. The constant τ was 180 ns at X-band and 200 ns at Q-band. T_m was measured by two-pulse echo-decay with a $\pi/2-\tau-\pi-\tau$ -echo sequence and two-step phase cycling. T_1 was measured by inversion recovery with a $\pi-T-\pi/2-\tau-\pi-\tau$ -echo sequence with variable T and two-step phase cycling. The constant τ in the inversion recovery pulse sequence was 200 ns at X-band and 360 ns at Q-band. Echo decays and inversion recovery curves were fitted with single exponentials.

DEER measurements and MMM simulations. The dipolar time evolution data was obtained at 83 or 150 K using a standard DEER four-pulse protocol, $(\pi/2)\text{mw1}-\tau_1-(\pi)\text{mw1}-\tau_1-(\pi)\text{mw2}-\tau_2-(\pi)\text{mw1}-\tau_2-\text{echo}$,¹⁸ on a Bruker 580 pulsed EPR spectrometer operating at Q-band frequency (33.9 GHz). All pulses were square pulses with lengths of 12, 24, and 40 ns, for $(\pi/2)\text{mw1}$, $(\pi)\text{mw1}$, and $(\pi)\text{mw2}$, respectively. Distance distributions were obtained from the time evolution data by assuming that the distance distribution can be approximated by a sum of Gaussians,^{19,20} including Gaussian distance distributions with 95% confidence bands.²¹ Simulation of distance distributions for the DZD-T4L were carried out on 2LZM in MMM2018 and for the DZD-T4L with β -CD in MMM2019.^{22,23}

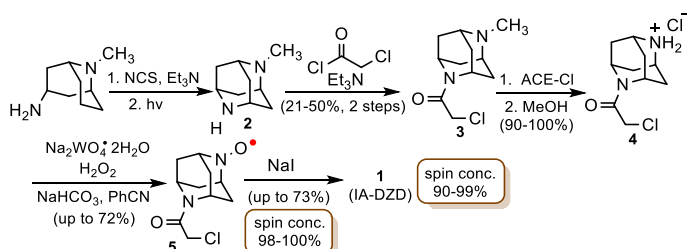
Results and Discussion

2,6-Diazaadamantane (DZD) is a promising framework for a spin label, as it provides the possibility of maintaining small molecular size with the required functionalization. The

construction of the adamantane framework requires laborious synthesis,^{10,24} and the synthesis of adamantane nitroxide spin label is complicated by the substituent group required for SDSL.

With *endo*-3-amino-9-methyl-9-azabicyclo[3.3.1]nonane, as a starting material, modified Hofmann–Löffler–Freytag (HLF) reaction with *N*-chlorosuccinimide (NCS)²⁵ and triethylamine provides **2** in isolated yields of up to 87% (Scheme 1).^{24b} Chloroacetyl chloride is added to the crude mixture of **2** in the presence of triethylamine, to produce **3** in 21 – 50% isolated yields (for two steps); the relatively low yield of **3** is ascribed to decomposition during purification. Subsequent de-methylation of **3** with 1-chloroethyl chloroformate (ACE-Cl) proceeds smoothly to **4** in >90% yield.²⁶ Initial attempts to oxidize **4** to **5** using common reagents, such as *meta*-chloroperbenzoic acid (*m*-CPBA) or H₂O₂ in the presence of catalytic amounts of Na₂WO₄, under a wide range of conditions, fail to provide nitroxide radical. Application of the Rosen/Payne method,²⁷ which employs acetonitrile as co-reactant in combination with H₂O₂, Na₂WO₄, and NaHCO₃ in methanol/water, provides **5** in low yields. We improved the yield of **5** up to about 70% by the replacement of acetonitrile with benzonitrile, presumably because the electron withdrawing phenyl group makes the key intermediate – peroxycarboximidic acid – more reactive. Finally, the reaction of **5** with NaI in dry acetone gives the spin label **1** (IA-DZD).

Scheme 1. Synthesis of IA-DZD Spin Label.



X-ray crystallography confirms the structure of **1** (Figure 2). In the crystal, the nitroxide has a pyramidalization angle $\theta_P = 10.69^\circ$ at the nitrogen atom, as determined by the POAV method.²⁸

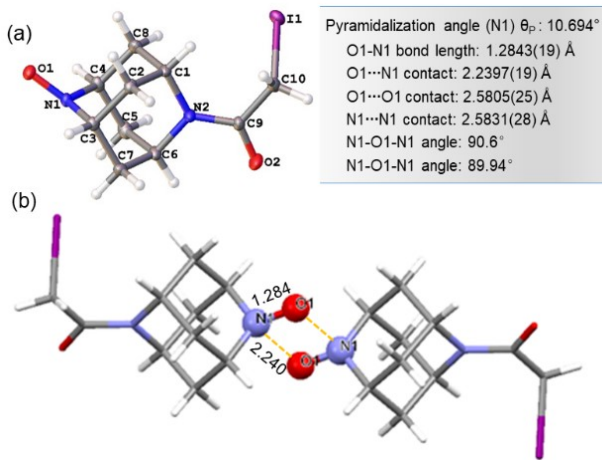


Figure 2. Molecular structure and conformation of **1** at 173 K. a) Ortep plot for **1**, with carbon, nitrogen, oxygen, and iodine atoms depicted with thermal ellipsoids set at the 50% probability level. b) Dimer structure of **1** with NO moieties emphasized as ball-and-stick and N-O distances (Å) within the dimer. See: SI, Tables S1 – S3, and Figs. S1 and S2, for details.

The iodine is gauche with respect to nitrogen N2, with the corresponding torsion angle N2-C9-C10-I1 = $-71.7(2)^\circ$. Notably, nitroxide **1** forms a head-to-tail NO π -dimer.²⁹ In the C_i -symmetric dimer structure, two NO moieties form an exact parallelogram (an approximate rectangle) with the N-O bond lengths of 1.284 Å and O1...N1 contacts of 2.240 Å (Figure 2). The O1...N1 contacts in the dimer of **1** correspond to only 73% of the O–N van der Waals contact of 3.07 Å,³⁰ and to our knowledge, are the shortest O...N contacts reported to date, thus implying very strong antiferromagnetic coupling between nitroxides.²⁹

We carried out a density functional theory (DFT) study of **5**, as it is computationally less demanding than spin label **1**.³¹ Geometry optimization of **5** at the UB3LYP/6-31G(d,p)+ZPVE level gives the C_s -symmetric conformation with pyramidal NO moiety and with *trans* orientation of the NO and carbonyl (CO) oxygens as a global minimum on the potential energy surface (PES). Another *N*-inverted, C_s -symmetric conformation with *cis* orientation of the NO and CO oxygens

is a local minimum that is about 0.2 kcal mol⁻¹ higher in energy. These two minima are connected by the transition state for inversion of configuration at the NO nitrogen; the barrier for the *N*-inversion is ~1.3 kcal mol⁻¹ (Table S14). The degree of pyramidalization at the nitrogen of the NO moiety is found to be similar to the X-ray determined geometry for the dimer of **1** and in all DFT-optimized minima for monomeric **5**; that is, inversion of configuration at the nitrogen of the NO moiety may be relevant to nitroxide spin labeled proteins.

The potential of **1** as a spin label for SDSL may be preliminarily evaluated from its hydrophobicity and molecular volume, based on the calculated partition coefficient and the Connolly solvent excluded volume (Supporting Information, Table S4). Nitroxide spin label **1** should minimally perturb the system of study, and thus is suitable for SDSL-DEER.

We explore the host–guest complexation of amine **3** with β -CD in D₂O by ¹H NMR spectroscopy, as described in detail in Supporting Information, Figs. S5–S12. The 1:1 stoichiometry of the complex is determined based on chemical shifts of the protons within the chloromethyl (ClCH₂) moiety in **3**, using the continuous variation method (Job plot).³² Significant upfield shifts of H-3' and H-5', which are located at the inner surface of β -CD, confirm the molecular complexation. In contrast, the chemical shift of H-6' at the narrow end of the cavity rim is also slightly changed, whereas H-1', H-2' and H-4' on the outside of the cavity are almost unaffected. The Benesi-Hildebrand plots provide the association constant, $K_a \approx 600 \text{ M}^{-1}$ at 311 K.³³ The ¹H-¹H ROESY spectrum of an equimolar mixture of **3** and β -CD shows cross-peaks that are consistent with the structure, in which the ClCH₂ moiety on **3** orients toward the narrow end of β -CD. This orientation of amine **3** (Figure 3) is consistent with a typical orientation of amino-adamantane guests inside the β -CD cavity.^{11c}

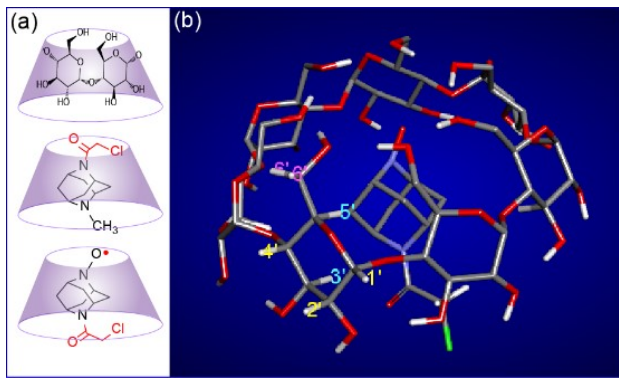


Figure 3. a) Schematic structures of major host-guest complexes of **3** and nitroxide **5** with β -CD, as determined by ^1H NMR spectroscopy. b) UB3LYP/6-31G(d) geometry of **5** complexed to β -CD; H1' – H6' on the β -CD are labeled.

We investigate complexation of nitroxide **5** with β -CD by ^1H NMR spectroscopy. Addition of β -CD to 0.5 mM **5** in D_2O leads to broadening and shifting of the resonances for H-3', H-6' and H-5' of the β -CD, while the chemical shift of protons of the chloromethyl group for **5** is almost unchanged (Fig. S13). This suggests that the chloromethyl group in **5** is closer to the wide end of β -CD (Figure 3a). We postulate that the orientation of **5** with the NO moiety pointing toward the narrow end of β -CD cavity may be facilitated by partial cancellation of dipole moments of **5** and β -CD;^{11c} UB3LYP/6-31(d)-computed dipole moments for **5**, β -CD, and the complex are 2.53 2.28, 1.31 D (Figure 3, Fig. S14 and Table S14). The association constants (K_a) with β -CD at 298 K in water are determined by isothermal titration calorimetry (ITC) as $K_a = 1090 \pm 8 \text{ M}^{-1}$ for **1** and $K_a = 755 \pm 7 \text{ M}^{-1}$ for **5**. In 0.11 M phosphate buffer, a comparable $K_a = 980 \pm 20 \text{ M}^{-1}$ is obtained for **1** (Table S8, Figs. S15–S17).

Our preliminary assessment of **1** in anhydrous trehalose/sucrose (9:1) matrix indicated T_m for **1** to be as expected for a spin label devoid of methyl groups, however, between 80 and 293 K, T_m

for **1** was similar in the presence and absence of β -CD.³⁴ In aqueous solution, the complexation of **1** with β -CD increased the rotational correlation time (τ_{rot}) of **1** by about a factor of 10.³⁴ CW EPR spectra of mono spin labeled DZD-T4L 135 at room temperature are clearly affected by the addition of β -CD, revealing the host-guest molecular recognition of DZD-nitroxide by β -CD; that is, τ_{rot} of 1.1 ns increases to 2.5 ns and isotropic hyperfine coupling constant $A(^{14}\text{N})$ decreases slightly (Figs. S18-S20, Tables S9-S10).^{35,36} The decrease in the isotropic hyperfine, attributed to a decrease in the tensor component, A_{zz} , based on simulations of the echo-detected spectra at 80 K, suggests a more hydrophobic environment for nitroxide inside β -CD. The increase in τ_{rot} suggests restriction of the range of motion that is accessible to the protein-bound spin label complexed with β -CD. Addition of β -CD to doubly spin labeled DZD-T4L 65/80 in 2:1 or 1:1 water/glycerol (w/g) in fluid solution caused broadening of CW EPR spectra, which suggests decreased mobility of the nitroxides. Because small-molecule nitroxides are known to form inclusion complexes with β -CD,³⁵ we carry out similar experiments using MTSL. Addition of β -CD to MTSL-T4L 65/135 or 65/80 in 2:1 or 1:1 w/g leads to spectral broadening due to decreased mobility of MTSL, presumably as a result of complexation with β -CD.

We obtain T_m and T_1 to provide additional insight into the host-guest molecular recognition of spin labeled T4L with β -CD (Table 1 and Figs. S21 and S22). In the presence of β -CD, at 80 and 160 K, T_m for IA-DZD in 1:1 w/g matrix increases by about 80%. For doubly labeled DZD-T4L in 2:1 w/g matrix, the analogous increase in T_m is in the 6–19% range, with the greatest increase (>10%) at higher temperatures, 150 or 160 K. Small change in T_1 upon binding of by β -CD does not significantly change the S/N for the DEER experiments; values of T_1 in 2:1 w/g are similar to those in trehalose matrix (Fig. S22, SI).

Table 1. Summary of T_m [μ s] and T_1 [μ s] for IA-DZD and DZD-T4L at \sim 35 GHz (Q-band) in Water/Glycerol (W/G) Matrix.^a

W/G Matrix	Sample	80 [K]		160 ^b [K]	
		T_m	T_1	T_m	T_1
1:1	IA-DZD	2.7	580	2.0	89
	IA-DZD+ β -CD	4.8	610	3.6	92
2:1	DZD-T4L 65/80	2.4	520	1.9 ^c	130 ^c
	DZD-T4L 65/80+ β -CD	2.6	420	2.2 ^c	110 ^c
	DZD-T4L 65/135	2.3	580	1.8	130
	DZD-T4L 65/135+ β -CD	2.4	530	2.0	110

^a Relaxation times are at the maximum amplitude peak in the echo-detected field-sweep spectra (Fig. S21, inset). Solutions contained 16 mM β -CD. Uncertainties are about 5% for T_m and about 10% for T_1 . ^b Relaxation times at 160 K unless otherwise noted. ^c Values at 150 K.

DEER distance measurements are carried out on the following doubly labeled DZD-T4L mutants: 65/80, 65/135, 59/159, and 61/128 in 2:1 w/g matrix without and with 10 mM β -CD at 83 and 150 K (Figure 4a, Table 2, Figs. S25, S27-S30). The mutants were selected, with cysteines at solvent accessible sites, to span C_β - C_β distances from 2.2 to 4.3 nm. Labeling of these mutants with IA-DZD was effective with efficiency up to 50% per cysteine. While the origin of the low labeling efficiency is unknown, it does not preclude our ability to accurately obtain distance distributions from these samples (Figs. S28 and S29). The main consequence of the labeling efficiency is the expected decrease in the depth of modulation. Selectivity of spin labeling is demonstrated by reaction of IA-DZD with T4L mutant without cysteines (T4L-cysless). CW EPR spectra show the spin-label to T4L-cysless ratio of 0.04, while the ratio for T4L 60/80 is 0.98 (0.49 per cysteine) (Fig. S26, SI); the low labeling of T4L-cysless is comparable with other spin-labels.

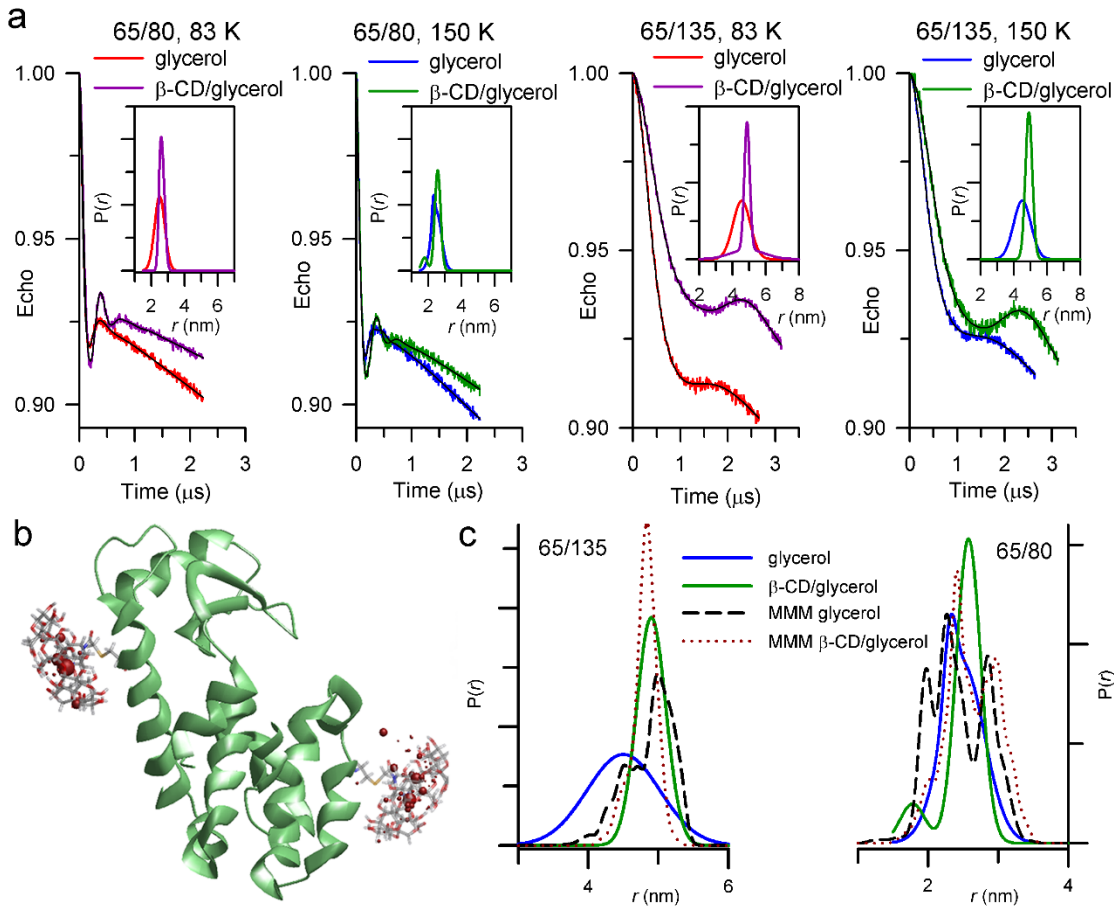


Figure 4. a) DEER distance measurements on doubly spin labeled DZD-T4L in 2:1 w/g matrix without and with 10 mM β -CD at 83 and 150 K. Main plots: normalized echo vs. time with fits where the distance distribution is a sum of Gaussians. Inset plots: distance distributions. b) Visualization of DZD/ β -CD rotamers at sites 65 (upper left) and 135 (lower right). The leading rotamer at each site is shown as stick model and the N-O bond midpoint of all rotamers as red spheres with volume proportional to rotamer population. c) Distance distributions for DZD-T4L: MMM computed vs. measured by DEER at 150 K without and with 10 mM β -CD. For additional details, see SI: Tables S11–S13, and Figs. S25–S40, including Gaussian distance distributions with 95% confidence bands.²¹

Upon addition of β -CD, the mean values of the DEER distance distributions shift to longer distances for all mutants; notably, the distance distributions become narrower, as measured by the standard deviation, σ (Table 2 and Figure 4a). For 65/80 and 65/135 mutants, we verify the distance distributions using Tikhonov regularization, which gives similar results, compared to the Gaussian fit (Table 2, Table S13, Figs. S33 and S34). Addition of β -CD to MTSL-T4L at 83 K leads to slight narrowing of distance distributions for 65/80 mutant; for 65/135 mutant, slight broadening of distance distributions with shift to longer distances are observed (Figs. S31 and S32).

Notably, DEER measurements for DZD-T4L 65/135 possess significantly higher sensitivity, compared to MTSL-T4L 65/135 (with and without β -CD), reflecting longer T_m for DZD-T4L (Table S12, SI).

Table 2. DEER and MMM Distance Distributions in 2:1 W/G Matrix.

T4L mutant	$C_\beta-C_\beta$ [nm]	MMM ^a DZD mean (σ) [nm]	MMM ^a DZD/ β -CD mean (σ) [nm]	Temp. [K]	DEER distances: mean (σ) [nm]				
					Gaussian fit			Tikhonov regularization	
					MTSL	DZD	DZD/ β -CD	DZD	DZD/ β -CD
65/80	2.23	2.44 (0.40)	2.62 (0.38)	83	2.60 (0.33)	2.50 (0.30)	2.64 (0.15)	2.49 (0.30)	2.62 (0.18)
				150	n/a	2.48 (0.30)	2.48 (0.31)	2.46 (0.26)	2.53 (0.25)
65/135	3.64	4.87 (0.34)	4.80 (0.19)	83	4.55 (0.31)	4.52 (0.52)	4.87 (0.16)	4.53 (0.48)	4.86 (0.35)
				150	n/a	4.50 (0.52)	4.90 (0.21)	4.47 (0.49)	4.82 (0.38)
59/159	3.36	4.40 (0.36)	4.24 (0.30)	83	4.19 (0.27) ^b	3.92 (0.51)	4.06 (0.48)	-	-
				150	n/a	3.75 (0.50)	4.04 (0.49)	-	-
61/128	4.34	5.24 (0.36)	5.29 (0.30)	83	4.62 (0.24) ^b	4.94 (0.70)	5.16 (0.59)	-	-
				150	n/a	4.99 (1.04)	5.24 (0.81)	-	-

^a Based on PDB structure 2LZM. ^b DEER distances for MTSL-T4L 59/159 and 61/128 were previously reported.³⁷

To compare the experimental inter-spin distance distributions with those expected from conformational variability of the spin label sidechain in T4L, MMM software is used to attach *in*

silico IA-DZD conformers from a rotamer library to the PDB structure of 2LZM T4L. The library of 216 rotamers for IA-DZD is generated using the approach that is similar to those used for other nitroxide- and Gd(III)-based spin labels:^{22,38} First, geometries for two minima of the DZD label with *Cys*-stub are optimized at the UB3LYP/def2-SVP level using ORCA³⁹ – two minima separated by 0.18 kcal mol⁻¹ are obtained, similar to nitroxide **5** at UB3LYP/6-31G(d,p) level (Fig. S35 and Table S14); second, rotamers of the linker between the protein backbone and the nitroxide fused ring structure are found by sampling conformation space at fixed bond lengths and angles using the torsion and non-binding interaction potentials of the UFF force field.⁴⁰ The resultant two 108-rotamer sets are combined by taking into account the energy difference of the minima for scaling populations according to Boltzmann distribution.

For DZD with β -CD, the rotamer library (Figure 4b) is generated from the UB3LYP/6-31G(d)-optimized geometry of methyl-sulfide-acetamide-DZD/ β -CD complex shown in SI, Fig. S14. To generate the *Cys*-stub, the initial structure of the DZD library is superimposed on atoms C9, N2, C1, and C6 (see: Figure 2a) onto the DZD/ β -CD structure (superposition rmsd 0.037 Å). Ensembles of 50,000 conformers are generated with forgive factors for van-der-Waals radii of 0.8, 0.85, 0.9, and 0.95 and libraries with 216 and 500 rotamers were generated for each forgive factor. Differences in predicted mean variances vary by less than 0.4 nm for any measured distance (typically 0.2 nm across all libraries). A forgive factor of 0.85 and 216 rotamers gives the best agreement with experiment.

The rotamer libraries for IA-DZD without and with β -CD are implemented in the MMM2018.1 and MMM2019.1 toolboxes.^{22,23} We observe good agreement between simulated and experimental mean distances in T4L when using IA-DZD with the rmsd between simulated and experimental mean distances lying in the range similar to MTSL (Table 2), where various approaches reproduce

mean distances with a standard deviation of 0.3 nm.⁴¹ Notably, DZD/β-CD experimental results show even better agreement with the DZD/β-CD library (Figure 4c). With the current rotamer libraries in MMM, the four mean distances measured at 80 K are predicted with mean deviations of 0.24, 0.33, and 0.11 nm for MTSL, DZD, and DZD/β-CD, respectively.

Conclusion

We have synthesized diazaadamantane-based iodoacetamide spin label **1** (IA-DZD) that is capable of host–guest molecular recognition with β-CD. IA-DZD forms 1:1 complex with β-CD in water, with an association constant, $K_a \approx 10^3 \text{ M}^{-1}$. The spin label could be doubly incorporated into T4L by SDSL with efficiency up to 50% per cysteine. The rigidity of the fused DZD ring structure and absence of mobile methyl groups decreases the temperature dependence of the spin echo dephasing time (T_m), which enables DEER distance measurement of distances $>4 \text{ nm}$ in DZD labeled-T4L in glycerol/water mixtures at temperatures up to 150 K. After addition of β-CD, the host–guest molecular recognition reduces the rotational correlation time of the label, slightly increases T_m , significantly narrows, and slightly lengthens the inter-spin distance distributions. DEER distance distributions, especially in the presence of β-CD, are in good agreement with simulated inter-spin distance distributions obtained by rotamer libraries for all studied mutants of DZD-T4L; in particular, the four mean distances for studied Cys-mutants measured at 80 K are predicted with mean deviation of 0.11 nm for DZD/β-CD vs. 0.24 nm for MTSL. The DEER data and the MMM calculations support the hypothesis that binding of β-CD to the DZD label restricts the range of accessible conformations of the label, which narrows the inter-spin distance

distributions. These results provide a foundation for developing supramolecular recognition to facilitate long-distance DEER measurements at near physiological temperatures.

ASSOCIATED CONTENT

Supporting Information

General procedures and materials, additional experimental details, X-ray crystallographic file for **1** in CIF format. This material is available free of charge via the Internet at <http://pubs.acs.org>.

AUTHOR INFORMATION

* Corresponding Authors

arajca1@unl.edu

hassane.mchaourab@Vanderbilt.Edu

sandra.eaton@du.edu

gjeschke@ethz.ch

Notes

The authors declare no competing financial interests.

ACKNOWLEDGMENT

We thank the National Institutes of Health (R01 GM124310-01 to AR, SR, SSE, and HM) and National Science Foundation (CHE-1665256 to AR) for support of this research. We thank Lukas Woodcock (University of Denver) for simulations of selected CW EPR spectra.

REFERENCES

(1) (a) Hubbell, W. L.; Lopez, C. J.; Altenbach, C.; Yang, Z. Technological Advances in Site-Directed Spin Labeling of Proteins. *Current Opinion Structural Biology* **2013**, *23*, 725–733; (b) Haugland, M. M.; Lovett, J. E.; Anderson, E. A. Advances in the Synthesis of Nitroxide Radicals for Use in Biomolecule Spin Labelling. *Chem. Soc. Rev.* **2018**, *47*, 668–680.

(2) Jeschke G. DEER Distance Measurements on Proteins. *Ann. Rev. Phys. Chem.* **2012**, *63*, 419–446.

(3) (a) Borbat, P. P.; Costa-Filho, A. J.; Earle, K. A.; Moscicki, J. K.; Freed, J. H. Electron spin resonance in studies of membranes and proteins. *Science* **2001**, *291*, 266–269. (b) Akyuz, N.; Georgieva, E. R.; Zhou, Z.; Stolzenberg, S.; Cuendet, M. A.; Khelashvili, G.; Altman, R. B.; Terry, D. S.; Freed, J. H.; Weinstein, H.; Boudker, O.; Blanchard, S. C. Transport domain unlocking sets the uptake rate of an aspartate transporter. *Nature* **2015**, *518*, 68–73.

(4) Borbat, P. P.; Georgieva, E. R.; Freed, J. H. Improved sensitivity for long-distance measurements in biomolecules: five-pulse double electron-electron resonance. *J. Phys. Chem. Lett.* **2013**, *4*, 170–175. (b) Srivastava, M.; Freed, J. H. Singular Value Decomposition Method to Determine Distance Distributions in Pulsed Dipolar Electron Spin Resonance. *J. Phys. Chem. Lett.* **2017**, *8*, 5648–5655.

(5) (a) Schmidt, T.; Wälti, M. A.; Baber, J. L.; Hustedt, E. J.; Clore, G. M. Long Distance Measurements up to 160 Å in the GroEL Tetradecamer Using Q-Band DEER EPR Spectroscopy. *Angew. Chem. Int. Ed.* **2016**, *55*, 15905–15909; (b) Dastvan, R.; Mishra, S.; Peskova, Y. B.; Nakamoto, R. K.; Mchaourab, H. S. Mechanism of Allosteric Modulation of P-Glycoprotein by Transport Substrates and Inhibitors. *Science* **2019**, *364*, 689–692.

(6) (a) Joseph, B.; Sikora, A.; Cafiso, D. S. Ligand Induced Conformational Changes of a Membrane Transporter in *E. coli* Cells Observed with DEER/PELDOR. *J. Am. Chem. Soc.* **2016**, *138*, 1844–1847; (b) Barth, K.; Hank, S.; Spindler, P. E.; Prisner, T. F.; Tampé, R.; Joseph, B. Conformational Coupling and *trans*-Inhibition in the Human Antigen Transporter Ortholog TmrAB Resolved with Dipolar EPR Spectroscopy. *J. Am. Chem. Soc.* **2018**, *140*, 4527–4533.

(7) Berliner, L. J.; Grunwald, J.; Hankovszky, H. O.; Hideg, K. A Novel Reversible Thiol Specific Spin Label: Papain Active Site Labeling and Inhibition. *Anal. Biochem.* **1982**, *119*, 450–455.

(8) (a) Dzuba, S. A.; Maryasov, A. G.; Salikhov, K. M.; Tsvetkov, Yu. D. Superslow rotations of nitroxide radicals studied by pulse EPR spectroscopy. *J. Magn. Reson.* **1984**, *58*, 95–117; (b) A. Zecevic, G. R. Eaton, S. S. Eaton, and M. Lindgren. Dephasing of electron spin echoes for nitroxyl radicals in glassy solvents by non-methyl and methyl protons. *Mol. Phys.* **1998**, *95*, 1255–1263; (c) Rajca, A.; Kathirvelu, V.; Roy, S. K.; Pink, M.; Rajca, S.; Sarkar, S.; Eaton, S. S.; Eaton, G. R. A Spirocyclohexyl Nitroxide Amino Acid Spin Label for Pulsed EPR Spectroscopy Distance Measurements. *Chem. Eur. J.* **2010**, *16*, 5778–5782; (d) Huang, S.; Paletta, J. T.; Elajaili, H.; Huber, K.; Pink, M.; Rajca, S.; Eaton, G. R.; Eaton, S. S.; Rajca, A. Synthesis and Electron Spin Relaxation of Tetracarboxylate Pyrroline Nitroxides. *J. Org. Chem.* **2017**, *82*, 1538–1544.

(9) (a) Meyer, V.; Swanson, M. A.; Clouston, L. J.; Boratyński, P. J.; Stein, R. A.; Mchaourab, H. S.; Rajca, A.; Eaton, S. S.; Eaton, G. R. Room-temperature distance measurements of immobilized spin-labeled protein by DEER/PELDOR. *Biophys. J.* **2015**, *108*, 1213–1219; (b) Krumkacheva, O.; Bagryanskaya, E. EPR-based distance measurements at ambient temperature. *J. Magnetic Reson.* **2017**, *280*, 117–126.

(10) (a) Dupeyre, R.-M.; Rassat, A.; Ronzaud, J. Nitroxides. LII. Synthesis and Electron Spin Resonance Studies of *N,N'*-Dioxy-2,6-diazaadamantane, a Symmetrical Ground State Triplet. *J.*

Am. Chem. Soc. **1974**, *96*, 6559–6568; (b) Dupeyre, R.-M.; Rassat, A. Nitroxydes LXXIII: Oxydation d'amines secondaires et tertiaires par le permanganate de potassium en milieu basique. *Tetrahedron Lett.* **1975**, *16*, 1839–1840; (c) Iwabuchi, Y. Discovery and Exploitation of AZADO: The Highly Active Catalyst for Alcohol Oxidation. *Chem. Pharm. Bull.* **2013**, *61*, 1197–1213.

(11) (a) Connors, K. A. The Stability of Cyclodextrin Complexes in Solution. *Chem. Rev.* **1997**, *97*, 1325–1358; (b) Wanka, L.; Iqbal, K.; Schreiner, P. R. The Lipophilic Bullet Hits the Targets: Medicinal Chemistry of Adamantane Derivatives. *Chem. Rev.* **2013**, *113*, 3516–3604; (c) Schönbeck, C. Charge Determines Guest Orientation: A Combined NMR and Molecular Dynamics Study of β -Cyclodextrins and Adamantane Derivatives. *J. Phys. Chem. B.* **2018**, *122*, 4821–4827.

(12) Krumkacheva, O.; Tanabe, M.; Yamauchi, S.; Fedin, M.; Marque, S. R. A.; Bagryanskaya, E. Time-Resolved and Pulse EPR Study of Triplet States of Alkylketones in β -Cyclodextrin. *Appl. Magn. Reson.* **2012**, *42*, 29–40.

(13) SAINT v. 2018.1, Bruker AXS, Madison, WI, 2018.

(14) SADABS v. 2018.1, Bruker AXS, Madison, WI, 2018.

(15) (a) Sheldrick, G. M. SHELXT – Integrated space-group and crystal-structure determination. *Acta Cryst. A* **2015**, *71*, 3 – 8. (b) Sheldrick, G. M. Crystal structure refinement with SHELXL. *Acta Cryst. C* **2015**, *71*, 3–8.

(16) Matthews B. W. Structural and genetic analysis of the folding and function of T4 lysozyme. *FASEB Journal* **1996**, *10*, 35–41.

(17) Mchaourab H. S.; Lietzow M. A.; Hubbell W. L. Motion of spin-labeled side chains in T4 lysozyme. Correlation with protein structure and dynamics. *Biochemistry* **1996**, *35*, 7692–7704.

(18) Pannier, M.; Veit, S.; Godt, A.; Jeschke, G.; Spiess, H. W. Dead-time free measurement of dipole-dipole interactions between electron spins. *J. Magn. Reson.* **2000**, *142*, 331–340.

(19) Brandon, S.; Beth, A. H.; Hustedt, E. J. The global analysis of DEER data. *J. Magn. Reson.* **2012**, *218*, 93–104.

(20) Stein, R. A.; Beth, A. H.; Hustedt, E. J. A Straightforward Approach to the Analysis of Double Electron-Electron Resonance Data. *Methods in Enzymology* **2015**, *563*, 531–567.

(21) Hustedt, E. J.; Marinelli, F.; Stein, R. A.; Faraldo-Gómez, J. D.; Mchaourab, H. S. Confidence Analysis of DEER Data and Its Structural Interpretation with Ensemble-Biased Metadynamics. *Biophys. J.* **2019**, *115*, 1200–1216.

(22) Jeschke, G. MMM: A toolbox for integrative structure modeling. *Protein Sci.* **2018**, *27*, 76–85.

(23) MMM2019.1: <https://www.polybox.ethz.ch/index.php/s/3yRTZKBhh8vzPg3/download>

(24) (a) Li, G.; Nelsen, S. F.; Jalilov, A. S.; Guzei, I. A. O-Capped Heteroadamantyl-Substituted Hydrazines and Their Oxidation Products. *J. Org. Chem.* **2010**, *75*, 2445–2452; (b) Darout, E.; Robinson, R. P.; McClure, K. F.; Corbett, M.; Li, B.; Shavnya, A.; Andrews, M. P.; Jones, C. S.; Li, Q. F.; Minich, M. L.; Mascitti, V.; Guimaraes, C. R. W.; Munchhof, M. J.; Bahnck, K. B.; Cai, C. M.; Price, D. A.; Liras, S.; Bonin, P. D.; Cornelius, P.; Wang, R. D.; Bagdasarian, V.; Sobota, C. P.; Hornby, S.; Masterson, V. M.; Joseph, R. M.; Kalgutkar, A. S.; Chen, Y., Design and Synthesis of Diazatricyclodecane Agonists of the G-Protein-Coupled Receptor 119. *J. Med. Chem.*

2013, 56, 301–319; (c) Zhang, J.; Hou, T.; Zhang, L.; Luo, J. 2,4,4,6,8,8-Hexanitro-2,6-diazaadamantane: A High-Energy Density Compound with High Stability. *Org. Lett.* 2018, 20, 7172–7176.

(25) Kimura, M.; Yoshio B., A Synthesis of 1,3-Diaza Heterocycles. A Hofmann-Loeffler Type of Photocyclization in the Absence of Strong Acid. *Synthesis* 1976, 3, 201–202.

(26) Olofson, R. A.; Martz, J. T.; Senet, J. P.; Piteau, M.; Malfroot, T., A new reagent for the selective, high-yield N-dealkylation of tertiary amines: improved syntheses of naltrexone and nalbuphine. *J. Org. Chem.* 1984, 49, 2081–2082.

(27) (a) Payne, G. B.; Williams, P. H., Reactions of Hydrogen Peroxide. VI. Alkaline Epoxidation of Acrylonitrile. *J. Org. Chem.* 1961, 26, 651–659; (b) Rauckman, E. J.; Rosen, G. M.; Aboudonia, M. B. Improved Methods for the Oxidation of Secondary Amines to Nitroxides. *Synthetic Commun.* 1975, 5, 409–413.

(28) Haddon, R. C. Comment on the Relationship of the Pyramidalization Angle at a Conjugated Carbon Atom to the σ -Bond Angles. *J. Phys. Chem. A.* 2001, 105, 4164–4165.

(29) (a) Howie, R. A.; Glasser, L. S. D.; Moser, W. Nitrosodisulphonates. Part 112 Crystal Structure of the Orange-Brown Triclinic Modification of Fremy's Salt (Potassium Nitrosodisulphonate). *J. Chem. Soc. A.* 1968, 3043–3047; (b) Rajca, A.; Pink, M.; Rojsajjakul, T.; Lu, K.; Wang, H.; Rajca, S. X-ray Crystallography and Magnetic Studies of a Stable Macroyclic Tetranitroxide. Intramolecular Dimer of Nitroxides in a Constrained Geometry of the Upper Rim of Calix[4]arene. *J. Am. Chem. Soc.* 2003, 125, 8534–8538; (c) Matsumoto S.; Higashiyama T.; Akutsu H.; Nakatsuji S. A Functional Nitroxide Radical Display Unique Thermochromism and

Magnetic Phase Transition. *Angew. Chem. Int. Ed.* **2011**, *50*, 10879–10883; (d) Preuss, K. E. Pancake bonds: π -Stacked dimers of organic and light-atom radicals. *Polyhedron* **2014**, *79*, 1–15.

(30) Bondi, A. Van der Waals Volumes and Radii. *J. Phys. Chem.* **1964**, *68*, 441–451.

(31) Frisch, M. J.; Trucks, G. W.; Schlegel, H. B.; Scuseria, G. E.; Robb, M. A.; Cheeseman, J. R.; Scalmani, G.; Barone, V.; Mennucci, B.; Petersson, G. A.; Nakatsuji, H.; Caricato, M.; Li, X.; Hratchian, H. P.; Izmaylov, A. F.; Bloino, J.; Zheng, G.; Sonnenberg, J. L.; Hada, M.; Ehara, M.; Toyota, K.; Fukuda, R.; Hasegawa, J.; Ishida, M.; Nakajima, T.; Honda, Y.; Kitao, O.; Nakai, H.; Vreven, T.; Montgomery, Jr., J. A.; Peralta, J. E.; Ogliaro, F.; Bearpark, M.; Heyd, J. J.; Brothers, E.; Kudin, K. N.; Staroverov, V. N.; Kobayashi, R.; Normand, J.; Raghavachari, K.; Rendell, A.; Burant, J. C.; Iyengar, S. S.; Tomasi, J.; Cossi, M.; Rega, N.; Millam, N. J.; Klene, M.; Knox, J. E.; Cross, J. B.; Bakken, V.; Adamo, C.; Jaramillo, J.; Gomperts, R.; Stratmann, R. E.; Yazyev, O.; Austin, A. J.; Cammi, R.; Pomelli, C.; Ochterski, J. W.; Martin, R. L.; Morokuma, K.; Zakrzewski, V. G.; Voth, G. A.; Salvador, P.; Dannenberg, J. J.; Dapprich, S.; Daniels, A. D.; Farkas, Ö.; Foresman, J. B.; Ortiz, J. V.; Cioslowski, J.; Fox, D. J. *Gaussian 09*, Revision A.1 (Gaussian, Inc., Wallingford CT, 2009).

(32) Ulatowski, F.; Dąbrowa, K.; Bałakier, T.; Jurczak, J. Recognizing the Limited Applicability of Job Plots in Studying Host–Guest Interactions in Supramolecular Chemistry. *J. Org. Chem.* **2016**, *81*, 1746–1756.

(33) Fielding, L. Determination of Association Constants (K_a) from Solution NMR Data. *Tetrahedron* **2000**, *56*, 6151–6170.

(34) Eaton, S. S.; Rajca, A.; Yang, Z.; Eaton, G. R. Azaadamantyl nitroxide spin label: complexation with β -cyclodextrin and electron spin relaxation. *Free Rad. Res.* **2018**, *52*, 319–326.

(35) (a) Martinie, J.; Michon, J.; Rassat, R. Nitroxides. LXX. Electron Spin Resonance Study of Cyclodextrin Inclusion Compounds. *J. Am. Chem. Soc.* **1975**, *97*, 1818–1823; (b) Franchi, P.; Lucarini, M.; Pedulli, G. F. Detection of Paramagnetic pH-Dependent Inclusion Complexes between β -Cyclodextrin Dimers and Nitroxide Radicals. *Angew. Chem. Int. Ed.* **2003**, *42*, 1842–1845; (c) Tan, X.; Song, Y.; Liu, H.; Zhong, Q.; Rockenbauer, A.; Villamena, F. A.; Zweier, J. L.; Liu, Y. Supramolecular host-guest interaction of trityl-nitroxide biradicals with cyclodextrins: modulation of spin-spin interaction and redox sensitivity. *Org. Biomol. Chem.* **2016**, *14*, 1694–1701.

(36) Stoll, S.; Schweiger, A. EasySpin, a comprehensive software package for spectral simulation and analysis in EPR. *J. Magn. Reson.* **2006**, *178*, 42–55.

(37) Alexander, N. S.; Stein, R. A.; Koteiche, H. A.; Kaufmann, K. W.; Mchaourab, H. S.; Meiler, J. RosettaEPR: rotamer library for spin label structure and dynamics. *PLoS One* **2013**, *8*, e72851.

(38) (a) Polyhach, Y.; Bordignon, E.; Jeschke, G. Rotamer libraries of spin labelled cysteines for protein studies. *Phys. Chem. Chem. Phys.* **2011**, *13*, 2356–2366; (b) Joseph B.; Sikora, A.; Bordignon, E.; Jeschke, G.; Cafiso, D. S.; Prisner, T. F. Distance Measurement on an Endogenous Membrane Transporter in *E. coli* Cells and Native Membranes Using EPR Spectroscopy. *Angew. Chem. Int. Ed.* **2015**, *54*, 6196–6199; (c) Bleicken, S.; Assafa, T. E.; Zhang, H.; Elsner, Ch.; Ritsch, I.; Pink, M.; Rajca, S.; Jeschke, G.; Rajca, A.; Bordignon, E. *gem*-Diethyl Pyrroline Nitroxide Spin Labels: Synthesis, EPR Characterization, Rotamer Libraries and Biocompatibility. *ChemistryOpen* **2019**, *8*, 1057–1065.

(39) Neese, F. The ORCA program system. *Wiley Interdisciplinary Reviews: Comp. Mol. Sci.* **2012**, *2*, 73–78.

(40) Rappe, A. K.; Casewit, C. J.; Colwell, K. S.; Goddard, W. A.; Skiff, W. M. UFF, a full periodic table force field for molecular mechanics and molecular dynamics simulations. *J. Am. Chem. Soc.* **1992**, *114*, 10024–10035.

(41) Jeschke, G. Conformational dynamics and distribution of nitroxide spin labels. *Prog. Nucl. Magn. Reson. Spectrosc.* **2013**, *72*, 42–60.

TOC GRAPHICS

